Original Article

Hyaluronan expression in primary and secondary brain tumors

Laurence Jadin[1], Sandra Pastorino[2], Rebecca Symons[1], Natsuko Nomura[2], Ping Jiang[1], Tiffany Juarez[2], Milan Makale[2], Santosh Kesari[2,3]

[1]Halozyme Therapeutics Inc., San Diego, CA, USA; [2]Translational Neuro-Oncology Laboratories, Moores Cancer Center, [3]Department of Neurosciences, UC San Diego, La Jolla, CA 92093, USA

Correspondence to: Santosh Kesari, MD, PhD. Translational Neuro-Oncology Laboratories, Moores Cancer Center, UC San Diego, 3855 Health Sciences Drive, MC 0819, La Jolla, CA 92093, USA. Email: skesari@ucsd.edu.

Background: Collectively, primary and secondary brain tumors represent a major public health challenge. Glioblastoma (GBM) is the most common primary brain tumor in adults and is associated with a dismal 5-year survival of only 10%. Breast cancer causes secondary tumors; it occurs in 200,000 patients yearly and 30% of these individuals develop brain metastases which also lead to a very poor prognosis. GBM and primary breast tumors are known to express hyaluronan (HA) which may serve as a therapeutic target.

Methods: For the present study we had two aims: (I) to identify suitable preclinical models for HA in GBM by examining HA expression in human GBM cell lines implanted orthotopically in mice; and (II) to determine whether breast cancer brain metastases in human patients express HA similar to the primary tumor. Forty human surgical samples of primary breast tumors and breast cancer brain metastases were processed and stained for HA. Athymic *nu/nu* mice were orthotopically implanted with one of 15 GBM lines and after tumors were established, quantitative immunohistochemistry determined whether.

Results: HA was expressed. All GBM cell lines and patient-derived orthotopic tumors did express HA, with 3 primary human lines expressing the highest staining intensity, above that of normal brain. All 40 human primary breast tumors and brain metastases examined also contained HA, though staining intensity was highly variable.

Conclusions: Our data support the use of specific patient-derived GBM cell lines in *nu/nu* mice for preclinical studies on HA-targeting therapies. Additionally, our research provides a basis for the assessment of HA expression and HA-targeting therapeutic agents for the treatment of breast cancer brain metastases.

Keywords: Hyaluronan (HA); breast cancer; glioblastoma (GBM); primary brain tumor; secondary brain tumor

Submitted Feb 13, 2015. Accepted for publication Mar 02, 2015.
doi: 10.3978/j.issn.2305-5839.2015.04.07
View this article at: http://dx.doi.org/10.3978/j.issn.2305-5839.2015.04.07

Introduction

Primary and secondary brain cancers have tremendous morbidity and poor outcomes. Glioblastoma (GBM) is the most common primary brain cancer in adults (1,2) and exhibits aggressive and invasive growth resulting in 13,000 deaths per year, with a median patient survival of 9-15 months (3). Secondary brain tumors, or metastases, occur in about 60,000 breast cancer patients per year, including those individuals with apparently well-controlled primary disease (4-7). This complication generally appears 2-3 years after the primary tumor diagnosis and almost always proves fatal.

From a therapeutic perspective, a potentially important finding is that GBM and primary breast tumors produce the extracellular matrix (ECM) component hyaluronan (HA), and these tumors also express elevated levels of the potentially oncogenic HA receptors CD44 and RHAMM (8-13). However, while previous reports have described HA expression in GBM, there is no comparative characterization of HA in a range of orthotopic animal models. In order to properly interpret results from such test systems, it is important to demonstrate that these tumor models express HA similarly to human GBM.

Although it is known that primary breast tumors contain HA, it is not known whether HA is expressed by breast

cancer metastases forming secondary tumors in the brain.

Filling this knowledge gap is critical given the promising early results obtained from targeting HA and CD44 in breast tumors and in pancreatic cancer (14). HA is a cell-surface-associated glycosaminoglycan that is ubiquitous in extracellular and pericellular matrices and exhibits a broad array of biological functions (15,16). In particular, HA is believed to impede access of chemotherapy agents to tumor cells, both by creating a physical barrier and acting as a molecular sieve (16,17). CD44 has been intensively studied in a range of cancers and it can drive multiple oncogenic signaling pathways when activated by HA (14-16). For example, several studies based on preclinical models of pancreatic cancer have indicated that enzymatic disruption of HA together with standard chemotherapy agents markedly improved antitumor efficacy (16). In a recent report, sustained enzymatic depletion of tumor HA with a pegylated recombinant human hyaluronidase PH20 (PEGPH20) decreased tumor interstitial fluid pressure (IFP) and water content, while significantly increasing vascular perfusion within HA-rich prostate PC3 tumors (18).

It is important to note that while human breast cancer metastases to the brain are generally treatment resistant, they do not infiltrate surrounding normal brain tissue beyond approximately 1 mm from metastatic sites (19). This suggests that if such foci can be ablated, possibly by combining cytotoxic therapy with hyaluronidase or a therapeutic agent targeting CD44/RHAMM signaling, a significant long-term reduction of the intracranial tumor burden may be achieved.

In the present work we evaluated HA levels in tumors from *nu/nu* mice inoculated intracranially with immortalized human GBM lines and primary patient-derived GBM lines. We found that all GBM tumors growing in the mouse brain expressed HA but the expression level was highly variable.

In addition we examined 40 human breast cancer surgical specimens of primary tumor and brain metastases and found that they all contained HA, and while the levels were generally comparable to normal human brain tissue, staining was quite varied.

These results provide a basis for further translational work in three contexts. First, the data support the use of specific patient-derived GBM cell lines in *nu/nu* mice as relevant models for preclinical studies incorporating HA-targeting therapeutics for the most common primary brain tumor in adults, GBM. Second, the demonstration of high HA expression in breast cancer brain metastases suggests the potential value of exploring therapeutic agents such as hyaluronidase and CD44/RHAMM signaling antagonists to enhance standard chemotherapy for breast tumor-derived secondary brain cancers. Finally the variable HA expression in patient-derived GBM tumors and human breast tumor brain metastases suggests that HA and HA-receptor related therapies may have to be considered on an individual basis depending on the levels of tumor HA.

Methods

Normal human brain and GBM surgical specimens

Normal human brain as formalin-fixed paraffin-embedded (FFPE) samples was acquired from autopsy material. GBM cell lines were acquired in two forms: either as commercially available immortalized serum dependent cell lines or as primary lines derived from human patient surgical samples. In the latter case GBM tissue specimens were obtained ethically with informed consent, according to an approved IRB protocol. The patient tumor samples were subjected to mechanical and enzymatic dissociation. The dissociated tissue was washed, filtered through a 30 μm mesh and plated onto ultra-low adherence flasks at a concentration of 500,000 to 1,500,000 viable cells/mL in stem cell isolation media containing human recombinant epidermal growth factor (EGF), human basic fibroblast growth factor (bFGF) and heparin and frozen for later use. The cells were thawed and cultured in suspension where they formed tumorspheres. All 15 immortalized and primary cell lines were concentrated from culture into a compact 2 μL volume, and stereotaxically inoculated into the right front cortex of *nu/nu* mice. Animal experimentation adhered to UCSD guidelines for animal research and was conducted in accordance with an approved IACUC protocol. The implanted tumor cells were allowed to grow for three weeks, following which the mice were euthanized, the brains excised, and sections prepared for H&E staining and histopathology.

Human breast tumors and breast tumor brain metastases

Under our UCSD IRB approved protocol, FFPE samples were acquired from clinical samples. Tissues included primary breast cancers and related brain metastases, or unrelated primary breast tumors and breast tumor brain metastases. All the metastases were acquired after treatment for the primary breast tumor, which may be presumed to have been standard although this could not be confirmed for all specimens.

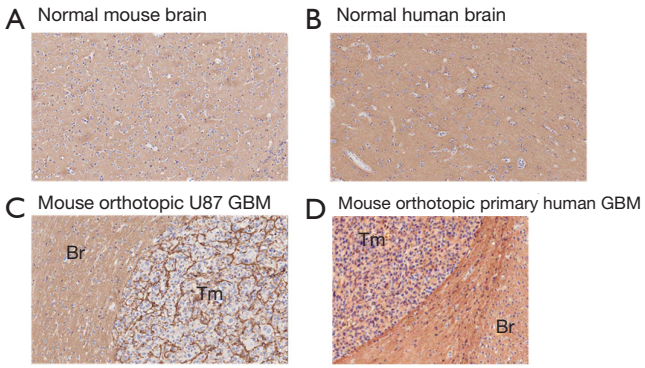

Figure 1 Histological HA-detection in normal mouse, human brain and a human GBM orthotopic tumor xenograft (20×). Photomicrographs of HA-stained normal mouse brain (A), human brain (B), a tumor mouse brain orthotopic xenograft derived from the U87 GBM immortalized cell line (C), and a brain orthotopic xenograft grown from a primary human GBM cell line (D). The tumor in panels C and D is indicated (Tm) along with normal brain (Br). HA (brown) was detected using biotinylated HABP followed by streptavidin-peroxidase and DAB, and Gill's hematoxylin (blue/purple) was used as a counterstain.

Staining methodology for paraffin embedded samples

The 4 µm paraffin sections were deparaffinized in xylene and rehydrated through graded ethanol (100-70%). Sections were treated in 25 mM PIPES, 70 mM NaCl, pH 5.5, with or without 100 µg/mL recombinant human PH20 (rHuPH20) hyaluronidase, for 2 h at 37 ℃. Sections were labeled with 2.5 µg/mL biotinylated HA-binding protein (EMD) overnight at 4 ℃. Normal brain or PC3 human prostate cancer cell line-derived xenografts were used as positive controls, while the hyaluronidase-treated slides served as negative controls. Detection was performed using streptavidin-HRP (BD) followed by DAB+ (Dako). Slides were counterstained with hematoxylin, coverslipped and representative micrographs were captured using an Axioskop (Zeiss) microscope equipped with a SPOT Pursuit camera (Diagnostic Instruments, Inc., Sterling Heights, MI, USA).

Assessment of HA staining

The stained sections were scanned using the digital Scanscope® XT scanner. The images were subsequently processed using ImageScope® software (Aperio Technology, Vista, CA, USA). All slides were scanned at an absolute magnification of 20× [resolution of 0.50 µm/pixel (50,000 pix/in.)]. The positive pixel count (PPC) algorithm was used to calculate staining positivity and strong positivity, represented by the ratio of pixels stained above a defined intensity threshold to the total number of pixels stained and counterstained, excluding white areas and expressed as a percentage. While we use the term "positivity" to include both medium and strongly stained positive pixels as determined by the algorithm, strong positivity refers to strongly stained pixels only.

Analysis

Staining intensity data were plotted using GraphPad Prism 5® (La Jolla, CA, USA) and analyzed with a one way analysis of variance (ANOVA) and the Wilcoxon-Mann-Whitney test comparing relative HA staining intensity.

Results

HA in human brain and in GBM cell lines grown in mouse brain

Human brain

Human brain generally showed higher HA staining intensity than mouse brain (*Figure 1* and *Figure 2A,B*). This variation may potentially represent a limitation of the *nu/nu* mouse brain tumor model for HA studies.

HA levels in 12 GBM orthotopic xenografts in the mouse

The HA levels in brain tumor cell lines grown in the mouse brain showed no systematic trend in that both the immortalized and patient-derived groups contained samples with comparatively high and low HA staining (*Figure 1C,D* and *Figure 2A,B*). An HA-stained section from a tumor grown in the mouse brain cortex is shown in *Figure 1C*. This tumor resulted from the implantation of a primary human GBM-derived cell line and it exhibited high HA staining intensity as did the adjacent normal brain tissue.

Virtually all established and patient-derived orthotopic tumor xenografts displayed variable staining intensity, as measured by the Aperio PPC algorithm and expressed as positivity (*Figure 2A*) or strong positivity (*Figure 2B*). Two GBM surgical specimens were also evaluated. Their positivity and strong positivity was in the range of what was measured for the GBM xenografts. The established, serum-dependent cell

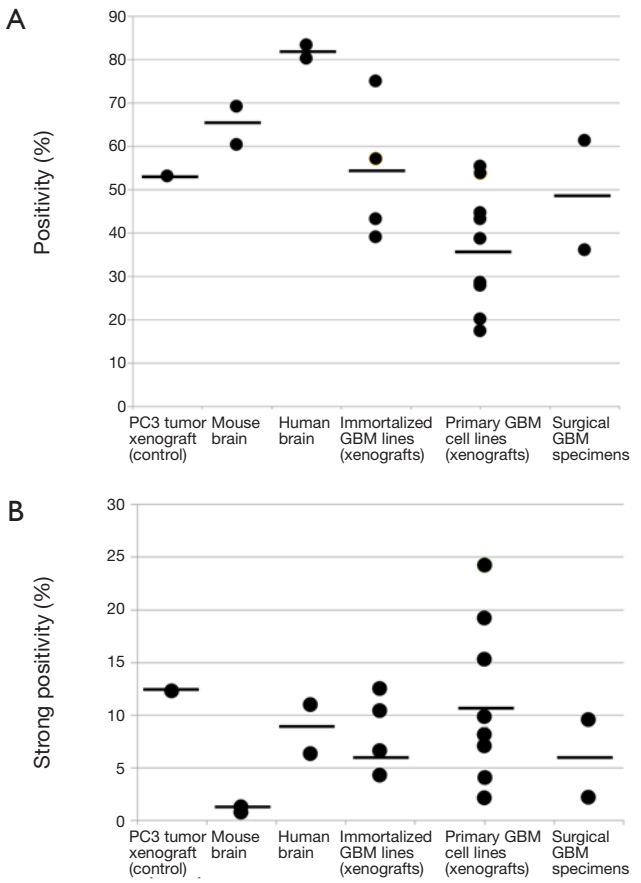

Figure 2 HA staining in GBM tumor xenografts orthotopically implanted in mouse brain. Scatterplot of HA staining positivity (A) and strong positivity (B) as measured in HABP-stained tissue sections using the Aperio positive pixel count, in a range of tumor xenografts derived from primary and immortalized GBM cell lines, compared with mouse brain, human brain, human (PC3) prostate cancer, and GBM surgical specimens. The mean value for each group is indicated by the horizontal line. No statistically significant difference was found between groups at the 5% level of confidence (unpaired parametric and non-parametric *t*-test).

line (U87, U251, LN382) derived tumors showed comparatively lower positivity, below that of normal human brain (*Figure 2A*). However, strong positivity was similar to that measured for normal human brain (*Figure 2B*). Three tumors grown from patient-derived (primary) GBM lines exhibited higher strong positivity than all other normal brain and brain tumor specimens (*Figure 2B*). These particular cell lines may be especially useful for preclinical studies to assess the efficacy of HA-depleting therapies in GBM.

HA levels in primary breast tumors and brain metastases

Initial assessment of HA staining with matched samples

We compared the intensity of HA staining in 7 patients for which primary breast cancer and matched brain metastases were available. *Figure 3* shows representative micrographs of primary breast tumors paired with their respective breast cancer brain metastases for each patient, all of which expressed HA, with a PC3 xenograft used as positive control. Staining positivity measurements are summarized in *Figure 4*. All primary breast tumors and brain metastases expressed HA, though the metastases had a lower positivity than their matched primary breast tumors (*Figure 4A*). Breast cancer brain metastases also exhibited high variability in HA staining, but in all 7 patients HA staining was present and the intensity in brain metastases was similar to or lower than their primary tumor (*Figure 4A*).

When plotting strong positivity *vs.* positivity for each matched pair of specimens, breast tumor samples had a greater proportion of both positive (P=0.004) and strongly positive pixels (P=0.0027) as compared with brain metastases (*Figure 4B*).

Expanded (unmatched) cohort assessment of HA staining

HA expression was further evaluated in another 5 primary breast tumors and 15 unmatched brain metastases from breast cancer patients. The intensity of staining in breast tumor brain metastases samples was variable and heterogeneous. This variability might be due to differences in tumor microenvironment, and/or grade of the brain metastasis. When plotting the positivity against the strong positivity for each sample (*Figure 5*), HA staining intensity of the majority of brain metastases was comparable or below that of primary breast tumors, and only 3 out of 15 brain metastases exhibited higher positivity than the 5 primary breast tumors.

Discussion

A growing literature shows that HA which is a major component of the extracellular matrix (ECM), may support the growth and invasion of several cancers by providing a scaffold for invasion and by interacting with specific receptors (15,18,20). HA signaling has been shown to promote oncogenic pathways and processes triggered by growth factors and matrix metalloproteinases (MMPs) (13,21,22).

HA is abundant in brain ECM, and primary gliomas

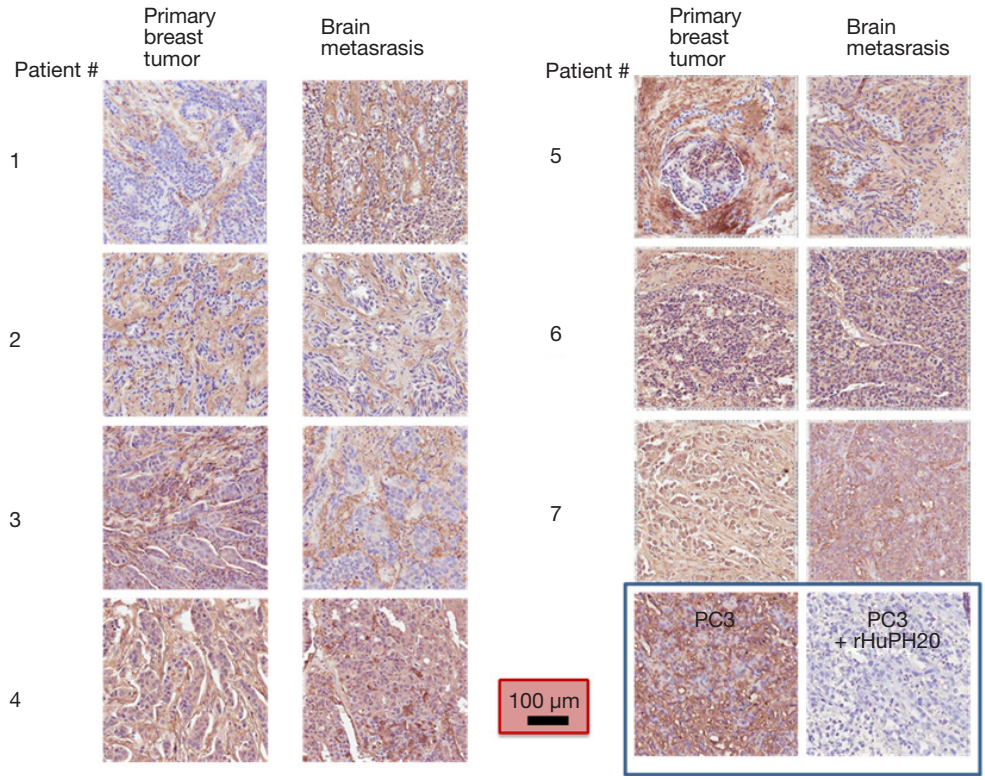

Figure 3 HA staining in primary breast cancers and matched brain metastases. Photomicrographs of HA-stained sections for 7 primary breast tumors paired with their matching brain metastasis. HA (brown) was detected using biotinylated HABP followed by streptavidin-peroxidase and DAB, and Gill's hematoxylin (blue/purple) was used as a counterstain. HA-stained sections of PC3 tumor xenograft, with and without rHuPH20 hyaluronidase pretreatment (to remove HA from the tissue section), were used as controls. Magnification for all the micrographs was ×20. The scale bar at bottom middle pertains to all images and corresponds to 100 microns.

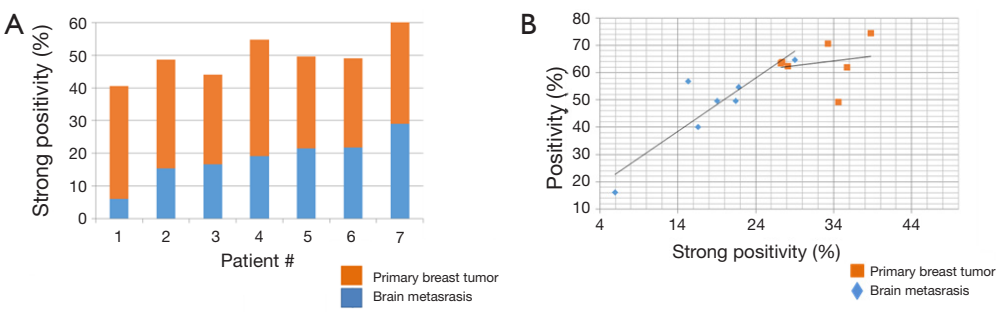

Figure 4 HA staining positivity in 7 primary breast tumors and matched brain metastases. (A) Histogram of HA staining positivity for each pair of primary breast cancer (orange bars) and matched brain metastasis (blue bars); (B) graph of HA staining positivity plotted against HA strong positivity. Metastases exhibited more variability than the primary breast tumors, and generally scored below primary breast tumors.

(including GBM) are known to express higher levels of HA than normal brain tissue (8,9). Glioma cells overexpress the HA receptors CD44 and RHAMM (12). Both receptors engage signaling molecules and downstream pathways that drive glioma migration and invasion (23). The tumor suppressor PTEN suppresses HA-induced invasion of U87 GBM cells and inactivating mutations of PTEN frequently occur in GBM (24,25). GBM depends on HA for expansion, and orthotopic mouse models derived from human cell lines that express relevant levels of HA, (i.e., express HA more

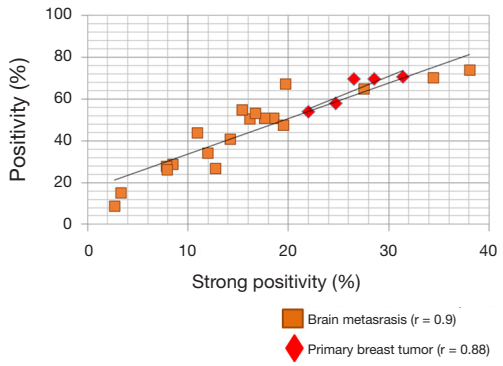

Figure 5 HA staining positivity in 5 primary breast tumors and 15 unmatched brain metastases. Linear graph of HA staining positivity versus strong positivity in primary breast tumors (red diamonds) and brain metastases (orange squares). The trend lines and r coefficients are indicated. Brain metastases generally displayed lower HA staining intensity than primary breast tumors, but with high variability. Only a minority of metastases exceeded primary breast tumor in terms of HA staining intensity.

than does normal human brain parenchyma) is essential for translational *in vivo* HA research in GBM (24). The present study tested 15 primary and immortalized GBM cell lines that were orthotopically implanted in the mouse and showed that several patient-derived GBM lines exhibited strongly positive HA staining that clearly exceeded that of normal human brain when grown in *nu/nu* mouse brain.

The identification of HA-producing patient-derived GBM tumor cell lines may be useful for preclinical studies designed to characterize HA and HA-targeting therapies in GBM. A correlation of the growth rate of the GBM cell lines with the intensity of HA staining will be the focus of a subsequent study.

Breast cancer is a major source of secondary brain tumors, and HA expression in breast primary tumors is associated with increased invasion and a poor prognosis (6,7,26). The analysis of both matched and unmatched breast tumor and brain metastasis samples showed that, while HA was present in all primary breast cancer and brain metastases, HA staining intensity was far more variable in metastases than in primary breast tumors. This may be relevant for selecting patients who may benefit from HA-targeted therapies. Moreover, it may be of interest to evaluate whether the expression of HA receptors, such as CD44, correlate with HA staining intensity. *In vitro*, CD44 orchestrates both pro- and anti-tumor signaling in breast cancer cells, while *in vivo* it can inhibit or drive metastasis (27). CD44 is physically linked, functionally coupled, and biosynthetically regulated with receptor tyrosine kinases, such as p185HER2 and non-receptor tyrosine kinases, e.g., c-Src family kinases (28,29). Interchain disulfide bonds link CD44 and p185HER2 and HA elicits CD44-associated p185HER2 tyrosine kinase signaling, driving tumor growth (28,30). Overexpression and amplification of HER2 oncogenes in breast cancer correlates with more aggressive tumor expansion and poor survival (31). Determination of tumor HA content may therefore hold prognostic and predictive value, and the pharmacologic modulation of HA levels may affect tumor expansion via CD44. The demonstration that breast cancer brain metastases express HA supports their use in further translational studies assessing the therapeutic targeting of HA, HA receptors, and associated signaling molecules.

In summary, this work represents an important first step in characterizing the relative levels of HA in GBM and in breast tumor brain metastases, supporting further research on HA as a potential biomarker for predicting response to HA and/or HA receptor-targeted therapies. We evaluated HA staining in orthotopic human GBM xenograft models, and we quantified HA in human breast cancer brain metastases. HA was present in all GBM tumor xenografts and was found to be elevated above the levels of normal human brain in some of the primary patient-derived GBM tumor xenografts. HA was also expressed in all primary breast tumors and their brain metastases, with high variability both between and within tumors. These initial data provide a foundation for more comprehensive investigations of the biology of HA in primary and secondary brain tumors. Such studies may help characterize HA as a biomarker to predict tumor response, evaluate hyaluronidase as a combination therapy to disrupt HA and improve access of chemotherapy drugs, and examine the effects of HA-CD44 signaling disruption on tumor progression.

Acknowledgements

Authors' contributions: L Jadin had key participation in conducting experiments and in data analysis. S Pastorino helped formulate study, conducted experiments and data analysis, prepared figures and contributed to writing manuscript. R Symons and P Jiang contributed to experiments and analysis. M Makale contributed to data analysis, figure preparation, and writing/editing the manuscript. T Juarez contributed to manuscript editing. S

Kesari formulated study idea and defined scientific context, examined and analyzed tissue sections, organized data and significantly edited/revised the manuscript.

Funding: This work was supported in part by a grant from NIH (NIH 3P30CA023100-25S8) to S Kesari. We thank Flagship Biosciences Inc., for scanning the tissue sections.

Disclosure: L Jadin, R Symons and P Jiang disclose that they are employees of Halozyme Therapeutics Inc.

References

1. Wen PY, Kesari S. Malignant gliomas in adults. N Engl J Med 2008;359:492-507.
2. Jones C, Perryman L, Hargrave D. Paediatric and adult malignant glioma: close relatives or distant cousins? Nat Rev Clin Oncol 2012;9:400-13.
3. Rulseh AM, Keller J, Klener J, et al. Long-term survival of patients suffering from glioblastoma multiforme treated with tumor-treating fields. World J Surg Oncol 2012;10:220.
4. Eichler AF, Loeffler JS. Multidisciplinary management of brain metastases. Oncologist 2007;12:884-98.
5. Gavrilovic IT, Posner JB. Brain metastases: epidemiology and pathophysiology. J Neurooncol 2005;75:5-14.
6. Gori S, Rimondini S, De Angelis V, et al. Central nervous system metastases in HER-2 positive metastatic breast cancer patients treated with trastuzumab: incidence, survival, and risk factors. Oncologist 2007;12:766-73.
7. Liu PH, Wang JD, Keating NL. Expected years of life lost for six potentially preventable cancers in the United States. Prev Med 2013;56:309-13.
8. Delpech B, Maingonnat C, Girard N, et al. Hyaluronan and hyaluronectin in the extracellular matrix of human brain tumour stroma. Eur J Cancer 1993;29A:1012-7.
9. Feng C, Zhang Y, Yin J, et al. Regulatory factor X1 is a new tumor suppressive transcription factor that acts via direct downregulation of CD44 in glioblastoma. Neuro Oncol 2014;16:1078-85.
10. Chen L, Bourguignon LY. Hyaluronan-CD44 interaction promotes c-Jun signaling and miRNA21 expression leading to Bcl-2 expression and chemoresistance in breast cancer cells. Mol Cancer 2014;13:52.
11. Klingbeil P, Natrajan R, Everitt G, et al. CD44 is overexpressed in basal-like breast cancers but is not a driver of 11p13 amplification. Breast Cancer Res Treat 2010;120:95-109.
12. Kim CS, Jung S, Jung TY, et al. Characterization of invading glioma cells using molecular analysis of leading-edge tissue. J Korean Neurosurg Soc 2011;50:157-65.
13. Hamilton SR, Fard SF, Paiwand FF, et al. The hyaluronan receptors CD44 and Rhamm (CD168) form complexes with ERK1,2 that sustain high basal motility in breast cancer cells. J Biol Chem 2007;282:16667-80.
14. Slomiany MG, Dai L, Tolliver LB, et al. Inhibition of Functional Hyaluronan-CD44 Interactions in CD133-positive Primary Human Ovarian Carcinoma Cells by Small Hyaluronan Oligosaccharides. Clin Cancer Res 2009;15:7593-601.
15. Toole BP. Hyaluronan-CD44 Interactions in Cancer: Paradoxes and Possibilities. Clin Cancer Res 2009;15:7462-8.
16. Whatcott CJ, Han H, Posner RG, et al. Targeting the tumor microenvironment in cancer: why hyaluronidase deserves a second look. Cancer Discov 2011;1:291-6.
17. Provenzano PP, Hingorani SR. Hyaluronan, fluid pressure, and stromal resistance in pancreas cancer. Br J Cancer 2013;108:1-8.
18. Thompson CB, Shepard HM, O'Connor PM, et al. Enzymatic depletion of tumor hyaluronan induces antitumor responses in preclinical animal models. Mol Cancer Ther 2010;9:3052-64.
19. Baumert BG, Rutten I, Dehing-Oberije C, et al. A pathology-based substrate for target definition in radiosurgery of brain metastases. Int J Radiat Oncol Biol Phys 2006;66:187-94.
20. Kosaki R, Watanabe K, Yamaguchi Y. Overproduction of hyaluronan by expression of the hyaluronan synthase Has2 enhances anchorage-independent growth and tumorigenicity. Cancer Res 1999;59:1141-5.
21. Yabushita H, Iwasaki K, Kanyama K, et al. Clinicopathological Role of Serum-Derived Hyaluronan-Associated Protein (SHAP)-Hyaluronan Complex in Endometrial Cancer. Obstet Gynecol Int 2011;2011:739150.
22. Montgomery N, Hill A, McFarlane S, et al. CD44 enhances invasion of basal-like breast cancer cells by upregulating serine protease and collagen-degrading enzymatic expression and activity. Breast Cancer Res 2012;14:R84.
23. Park JB, Kwak HJ, Lee SH. Role of hyaluronan in glioma invasion. Cell Adh Migr 2008;2:202-7.
24. Park MJ, Kim MS, Park IC, et al. PTEN suppresses hyaluronic acid-induced matrix metalloproteinase-9 expression in U87MG glioblastoma cells through focal adhesion kinase dephosphorylation. Cancer Res 2002;62:6318-22.
25. Gont A, Hanson JE, Lavictoire SJ, et al. PTEN loss

represses glioblastoma tumor initiating cell differentiation via inactivation of Lgl1. Oncotarget 2013;4:1266-79.
26. Heldin P, Basu K, Olofsson B, et al. Deregulation of hyaluronan synthesis, degradation and binding promotes breast cancer. J Biochem 2013;154:395-408.
27. Louderbough JM, Schroeder JA. Understanding the dual nature of CD44 in breast cancer progression. Mol Cancer Res 2011;9:1573-86.
28. Bourguignon LY, Zhu H, Chu A, et al. Interaction between the adhesion receptor, CD44, and the oncogene product, p185HER2, promotes human ovarian tumor cell activation. J Biol Chem 1997;272:27913-8.
29. Ai M, Liang K, Lu Y, et al. Brk/PTK6 cooperates with HER2 and Src in regulating breast cancer cell survival and epithelial-to-mesenchymal transition. Cancer Biol Ther 2013;14:237-45.
30. Fiszman GL, Jasnis MA. Molecular Mechanisms of Trastuzumab Resistance in HER2 Overexpressing Breast Cancer. Int J Breast Cancer 2011;2011:352182.
31. Tan GH, Choo WY, Taib NA, et al. Factors associated with HER2 overexpression in breast cancer: Experience in an Asian developing country. Asian Pac J Cancer Prev 2009;10:837-40.

Cite this article as: Jadin L, Pastorino S, Symons R, Nomura N, Jiang P, Juarez T, Makale M, Kesari S. Hyaluronan expression in primary and secondary brain tumors. Ann Transl Med 2015;3(6):80. doi: 10.3978/j.issn.2305-5839.2015.04.07

